

Metronidazole removal in powder-activated carbon and concrete-containing graphene adsorption systems: Estimation of kinetic, equilibrium and thermodynamic parameters and optimization of adsorption by a central composite design

S. V. Manjunath^a, S. Mathava Kumar^{a,*}, Huu Hao Ngo^b, and Wenshan Guo^b

^aDepartment of Civil Engineering, Indian Institute of Technology Madras, Chennai, Tamil Nadu, India;

^bSchool of Civil and Environmental Engineering, University of Technology Sydney, Sydney, Australia

* Corresponding authors. Mathava Kumar (mathav@iitm.ac.in; mathavakumar@gmail.com);
Department of Civil Engineering, Indian Institute of Technology Madras, Chennai 600036, Tamil Nadu, India.

Abstract

Metronidazole (MNZ) removal by two adsorbents, i.e., concrete-containing graphene (CG) and powder-activated carbon (PAC), was investigated via batch-mode experiments and the outcomes were used to analyze the kinetics, equilibrium and thermodynamics of MNZ adsorption. MNZ sorption on CG and PAC has followed the pseudo-second-order kinetic model, and the thermodynamic parameters revealed that MNZ adsorption was spontaneous on PAC and non-spontaneous on CG. Subsequently, two-parameter isotherm models, i.e., Langmuir, Freundlich, Temkin, Dubinin–Radushkevich and Elovich models, were applied to evaluate the MNZ adsorption capacity. The maximum MNZ adsorption capacities (q_m) of PAC and CG were found to be between 25.5–32.8 mg/g and 0.41–0.002 mg/g, respectively. Subsequently, the effects of pH, temperature and adsorbent dosage on MNZ adsorption were evaluated by a central composite design (CCD) approach. The CCD experiments have pointed out the complete removal of MNZ at a much lower PAC dosage by increasing the system temperature (i.e., from 20°C to 40°C). On the other hand, a desorption experiment has shown 3.5% and 1.7% MNZ removal from the surface of PAC and CG, respectively, which was insignificant compared to the sorbed MNZ on the surface by adsorption. The overall findings indicate that PAC and CG with higher graphene content could be useful in MNZ removal from aqueous systems.

Keywords: Adsorption, isotherm, kinetics, metronidazole, thermodynamics

1. Introduction

Pharmaceuticals constitute a diverse group of organic compounds and are considered to be one of the most important emerging contaminants in the recent years. These include different compounds such as antibiotics, hormones, analgesics and anti-inflammatory drugs, antiepileptic drugs, blood lipid regulators, β blockers, contrast media and cytostatic drugs.^[1] The usage of antibiotics has been increasing considerably day by day owing to the personal requirements of people, and demand in industries such as animal pharmaceuticals, aquaculture, poultries, piggeries, etc. The discharge of antibiotics into the environment could produce antimicrobial-resistant genes and they can also produce eco-toxicity.^[2] Antibiotics and/or their metabolites were found to have longer stability or half-life in aqueous and soil environments. Recent studies have reported the persistence of

antibiotics of different classes in aqueous environments^[3-5] and the release of antibiotics from wastewater treatment plant effluents.^[6,7] Metronidazole (MNZ), an antibacterial and anti-inflammatory agent,^[8] is one of the heavily used antibiotics worldwide,^[9] which has been used to treat diseases caused by anaerobic bacteria, bacteroides and protozoa. MNZ has very high solubility (9.8 g/L) and molecular diffusivity (8.48×10^6 cm²/s) in water, and is expected to be highly mobile in aqueous systems. Recently, Rosal et al.^[10] reported the presence of MNZ concentration in the influent (165 ng/L) and effluent (127 ng/L) samples of a sewage treatment plant.

The conventional wastewater treatment process relies mainly on the function of biological treatment units. However, these units are ineffective in the removal of a wide variety of antibiotics including MNZ.^[11] Therefore, it is vital to include appropriate technology (as a tertiary treatment) in the treatment process to remove the emerging contaminants including MNZ. Due to the increasing interest in the removal of antibiotics from aqueous systems, several researchers explored the possibility of MNZ removal by electrochemical process,^[12] photocatalysis,^[13] electro-catalytic reduction,^[14] membrane process,^[15] Fenton process^[16] and coupled electro-reduction-biological treatment,^[17] etc. However, adsorption, one of the oldest techniques, has been found to be very effective in the removal of a wide variety of trace and gross organics. Moreover, this process has been used extensively in the wastewater treatment process owing to its ease in operation, low cost, absence of by-product formation, regeneration potential and sludge-free operation when compared to other treatment methods.^[18,19]

Due to rapid and excessive urbanization, construction and demolition wastes have become a major concern in the context of urban solid waste management.^[20] The disposal of construction and demolition wastes has become one of the biggest concerns throughout the world, as it is generated in huge quantities. Landfilling of construction and demolition wastes is the main current practice in many developing countries. Moreover, it was reported that the wastes were dumped illegally on land or in natural drainages in most developing countries due to shortage of space for dumping. However, the construction and demolition wastes containing cementitious material can be reused or recycled for other processes/applications. Several investigations in the past reported the application of cementitious materials in the removal of various pollutants from water and wastewater including phosphorous by composite cement mortars;^[21] fecal coliforms and phosphorous by pervious geopolymer concrete;^[22] p-chloronitrobenzene by the cementitious catalytic membrane with ozonation;^[23] Indigo carmine by concrete composite;^[24] and heavy metals (Cu, Cd, Zn and Pb) by zeolite-Portland cement mixture.^[25]

In the recent years, graphene and graphene composites have been used as adsorbents to treat water and wastewater containing heavy metals, organic dyes and antibiotics. To mention a few, iron–aluminum oxide–graphene oxide composite for fluoride removal,^[26] graphene oxide for removing diclofenac and sulfamethoxazole antibiotics,^[27] polysaccharide-modified graphene oxides for the removal of cationic dyes (Methylene blue, Rhodamine 6G) and anionic dyes (Orange II, Acid fuchsin),^[28] and graphene oxide membranes for Cu²⁺, Cd²⁺ and Ni²⁺ removal are some examples.^[29] On the other hand, several investigations are in progress to study the addition of graphene/graphene oxide in the concrete preparation to increase its strength and other characteristics. The application of concrete prepared with the addition of graphene for water purification especially for antibiotics' removal has not been investigated. Moreover, the requirement/suitability of graphene content in

concrete for the effective removal of antibiotics was not addressed in the past. At the same time, it is essential to compare the performance of modified concrete with graphene with commercially available adsorbents including PAC which has huge importance in the application of modified concrete for water purification applications. On the other hand, the interaction effect of adsorbent dosage, pH and temperature on the removal of antibiotics using a central composite design (CCD) along with isotherm experiments was not carried out in the past. Therefore, this investigation was focused to evaluate the performance of concrete-containing graphene (CG) in MNZ removal and its effectiveness was compared with the MNZ removal potential of powdered activated carbon (PAC) by calculating the kinetic rates, thermodynamic parameters and adsorption capacity using isotherms. Moreover, this study was extended to explore (a) the interaction effects of temperature, pH and adsorbent dosage on MNZ removal and (b) the extent of MNZ desorption from CG and PAC.

2. Materials and methods

2.1. Preparation of adsorbent

PAC was supplied by Merck, India, and it was used without any modification. CG (2%w/w, 1–2 mm size) was obtained from the Building Technology and Construction Management laboratory of IIT Madras, India. Prior to the adsorption experiments, the CG specimen was crushed, and the particles retained between ASTM sieve Nos. 8 and 16 were collected and washed several times with tap water followed by distilled water. Subsequently, the particles were air-dried and stored in an airtight container for further use. The surface morphology of the adsorbents before and after adsorption was analyzed by using a scanning electron microscope (GENESIS-2100 SEM, EmCrafts, South Korea).

2.2. Preparation of adsorbate

MNZ ($C_6H_9N_3O_3$) of analytical grade supplied by Sigma-Aldrich was used for the preparation of stock solution (1,000 mg/L). The prepared stock solution was placed in a volumetric flask, sealed and stored in a refrigerator. The working solutions of required concentrations were prepared from the stock solution (1,000 mg/L) by diluting it with distilled water.

2.3. Kinetic and equilibrium adsorption study

2.3.1. Kinetic study

The kinetic study was conducted in a batch mode at an initial MNZ concentration of 10 mg/L. Exactly 100 mL of solution containing 10 mg/L MNZ was poured into 250-mL conical flasks, and the adsorbent (either PAC or CG) was added into the flasks at a predetermined adsorbate-to-adsorbent ratio (basis of wt:wt; 1:100 for PAC and 1:1,000 for CG). Subsequently, the flasks were kept in a temperature-controlled incubator shaker at 25°C with continuous shaking at 100 rpm for 24 h. At regular time intervals, the samples were withdrawn from the flasks and analyzed for MNZ concentration.

2.3.2. Equilibrium study

Batch-mode equilibrium adsorption experiments were conducted under similar operating conditions, i.e., at 25°C, 100-mL working volume with continuous shaking with a range of initial MNZ concentrations (5, 10, 25, 50 and 100 mg/L). The adsorbate-to-adsorbent ratio was fixed as 1:100 and 1:1,000 (on a wt:wt basis) for PAC and CG, respectively. The experiments were conducted for a pseudo-equilibrium time obtained from the kinetic study. At the end of the experiment, the samples were collected from the flasks and analyzed for MNZ concentration. Using the experimental data, MNZ adsorption capacity q_e (mg/g) at equilibrium was calculated as given in Eq. (1):

$$q_e = \frac{(C_o - C_e)V}{M} \quad (1)$$

where C_o and C_e are MNZ concentrations at the start of the experiment and at equilibrium (mg/L), respectively. V is the volume of MNZ solution (L) and M is the mass of adsorbent (g).

2.4. Quantification of MNZ concentration

After the adsorption study, an aliquot of MNZ solution was collected, centrifuged and filtered. Subsequently, the filtered sample was analyzed using high-performance liquid chromatography (HPLC) fitted with a UV-Vis variable wavelength detector (Dionex UltiMate 3000). The C18 chromatographic column (Acclaim 120, 5 μ m, 4.6 \times 250 mm) was used to separate the compounds. The column was operated at a reverse phase mode at a wavelength of 254 nm using acetonitrile:water (60:40) as a mobile phase. The pump was operated at a flow rate of 1 mL/min. The HPLC analysis results were used to calculate the MNZ removal as per Eq. (2):

$$\text{MNZ removal (\%)} = \left(\frac{C_o - C_e}{C_o} \right) * 100 \quad (2)$$

2.5. Determination of rate constants

The rate of adsorption was determined using the adsorption equilibrium data and equilibrium models (i.e., the pseudo-first-order and pseudo-second-order models).

Pseudo-first-order model

Lagergren's pseudo-first-order rate equation [Eq. (3)] describes the adsorption of liquid-solid systems based on the concentration of the solution and adsorption capacity of the solid. Equation (3) states that the rate of adsorption is equal to the distance to equilibrium. At time $t = 0$ for fresh adsorbent, $q_t = 0$ and the distance of equilibrium is q_e . The increase in time reduces the distance of equilibrium, while the distance disappears at equilibrium, i.e., $q_e - q_t = 0$.^[30] Equation (4) depicts the expression for the pseudo-first-order model in a linearized form:

$$\frac{dq}{dt} = K_1(q_e - q_t) \quad (3)$$

$$\ln(q_e - q_t) = \ln q_e - K_1 t \quad (4)$$

where q_e and q_t are adsorption capacities (mg/g) at equilibrium and at various times (t), respectively. K_1 is the pseudo-first-order rate constant (min^{-1}) that was obtained by plotting a graph of $\ln(q_e - q_t)$ versus t .

Pseudo-second-order model

The rate of pseudo-second-order reaction depends on the amount of adsorbate adsorbed on the adsorbent. The adsorption capacity at equilibrium is a function of temperature, adsorbent dosage, initial adsorbent concentration in solution and the nature of solute sorbent interaction.^[31] The pseudo-second-order model is based on the assumption that the rate-limiting step is chemisorption involving valency forces through sharing or exchange of electrons between the adsorbent and the adsorbate.^[32] The expressions for the pseudo-second-order model and the linearized form are given in Eqs. (5) and (6), respectively:

$$\frac{dq}{dt} = K_2(q_e - q_t)^2 \quad (5)$$

$$\frac{t}{q_t} = \frac{1}{K_2 q_e^2} + \frac{t}{q_e} \quad (6)$$

where K_2 is the pseudo-second-order rate constant (g/mg/min) and it was obtained by plotting a graph (t/q_t) versus t .

2.6. Adsorption isotherm

An adsorption isotherm represents the relationship between the amount of adsorbate adsorbed onto the surface of an adsorbent and the concentration of adsorbate in the solution at a constant temperature under the equilibrium condition.^[33] In this study, Langmuir, Freundlich, Temkin, Dubinin–Radushkevich and Elovich isotherm models were used to fit the experimental data.

Langmuir isotherm

The Langmuir isotherm model assumes that the adsorption is monolayer and takes place at specific homogeneous sites on the adsorbent. Once a pollutant occupies a site, no further adsorption can occur in that particular site, i.e., adsorbent has a finite capacity for the pollutant. There is no interaction between the molecules adsorbed onto the neighboring sites.^[34] The Langmuir isotherm is shown in Eq. (7):

$$q_e = \frac{q_m K_L C_e}{1 + K_L C_e} \quad (7)$$

Where q_e is the equilibrium adsorption capacity (mg/g), q_m is the Langmuir isotherm constant representing monolayer adsorption capacity (mg/g), C_e is the equilibrium concentration of MNZ in the solution (mg/L) and K_L is the Langmuir constant. Equation (8) shows the linearized form of Langmuir isotherm:

$$\frac{1}{q_e} = \frac{1}{q_m} + \frac{1}{q_m K_L C_e} \quad (8)$$

The Langmuir isotherm constants, i.e., K_L and q_m , are obtained by plotting a graph of $\frac{1}{q_e}$ vs $\frac{1}{C_e}$. Favorability of adsorption process is evaluated by a dimensionless parameter, i.e., separation or equilibrium parameter R_L , as shown in Eq. (9):

$$R_L = \frac{1}{1 + (K_L C_0)} \quad (9)$$

If R_L is $0 < R_L < 1$, the adsorption process is favorable, $R_L > 1$ indicates that adsorption is unfavorable, $R_L = 1$ indicates linear adsorption and $R_L = 0$ indicates that the adsorption process is irreversible in nature.

Freundlich isotherm

The Freundlich isotherm [Eq. (10)] is an empirical expression based on the assumption that the adsorbent has a heterogeneous surface composed of different classes of adsorption sites. This can be applied to multilayer adsorption, with a non-uniform distribution of adsorption heat and affinities over the heterogeneous surface.^[35]

$$q_e = K_F C_e^{\frac{1}{n}} \quad (10)$$

Where K_F is the Freundlich isotherm constant signifying adsorption capacity and $\frac{1}{n}$ is the Freundlich constant representing intensity of the adsorption or surface heterogeneity, revealing higher heterogeneity as it tends to 0. The value of Freundlich constant between 0 and 1 indicates favorable adsorption. Equation (11) shows the linearized form of Freundlich isotherm, and a plot of $\ln(q_e)$ versus $\ln(C_e)$ gives slope $\frac{1}{n}$ and intercept K_F .

$$\ln q_e = \ln K_F + 1/n \ln C_e \quad (11)$$

Temkin isotherm

The Temkin isotherm is based on the assumption that the heat of adsorption of all the molecules in a layer decreases linearly with a coverage due to adsorbent–adsorbate interactions. It mainly describes the chemical adsorption process as the one involving electrostatic interaction.^[36] Equations (12) and (13) represent the Temkin isotherm model and its linearized form, respectively:

$$q_e = B \ln(A_T C_e) \quad (12)$$

$$q_e = B \ln A_T + B \ln C_e \quad (13)$$

Where B is a constant related to heat of adsorption given by $B = \frac{RT}{\Delta Q}$ and A_T is the Temkin equilibrium-binding constant (L/mol). A plot of q_e versus $\ln(C_e)$ is used to estimate the slope B and intercept A_T .

Dubinin–Radushkevich isotherm

The Dubinin–Radushkevich isotherm model does not assume a homogeneous surface or a constant adsorption potential like the Langmuir model.^[37] Equations (14) and (15) represent the Dubinin–Radushkevich isotherm model and its linearized form, respectively. Slope and intercept of the plot $\ln(q_e)$ vs ε^2 give K_{DR} constant related to the mean free energy of adsorption (mol^2/kJ^2) and maximum adsorption capacity (q_m), respectively, where ε indicates the Polanyi potential given by Eq. (16). The mean free energy value (E) (kJ/mol) can be found by using K_{DR} values using Eq. (17). Any value of E less than 8 kJ/mol indicates that the adsorption is physical in nature, whereas the E value between 8 and 16 kJ/mol and greater than 16 kJ/mol indicates the adsorption by exchange of ions and chemisorption, respectively.^[38]

$$q_e = q_m \exp(-K_{DR}\varepsilon^2) \quad (14)$$

$$\ln q_e = \ln(q_m) - (K_{DR}\varepsilon^2) \quad (15)$$

$$\varepsilon = RT \ln \left[1 + \frac{1}{C_e} \right] \quad (16)$$

$$E = \left[\frac{1}{\sqrt{2K_{DR}}} \right] \quad (17)$$

Elovich isotherm

The Elovich isotherm model is based on the assumption that adsorption sites increase exponentially with adsorption, which implies a multilayer adsorption.^[39] Equations (18) and (19) represent the Elovich isotherm model and its linearized form, respectively. The slope and intercept of the plot $\ln(q_e/C_e)$ versus q_e give maximum adsorption capacity (q_m) and Elovich equilibrium constant (K_E in L/mg), respectively:

$$\frac{q_e}{q_m} = K_E C_e \exp \left[-\frac{q_e}{q_m} \right] \quad (18)$$

$$\ln \frac{q_e}{C_e} = \ln K_E q_m - \frac{1}{q_m} q_e \quad (19)$$

2.7. Estimation of thermodynamic parameters

Adsorption thermodynamics play a vital role in understanding adsorption mechanisms, i.e., physisorption or chemisorption. Thermodynamic parameters such as change in free energy (ΔG^0), enthalpy (ΔH^0) and entropy (ΔS^0) were used to determine the spontaneity, heat of change and randomness in the adsorption of MNZ using Eqs. (20)–(22), respectively:

$$\Delta G^0 = -RT \ln k_c \quad (20)$$

ΔG^0 is related to the change in enthalpy and entropy given by Eq. (21):

$$\Delta G^0 = \Delta H^0 - T\Delta S^0 \quad (21)$$

The entropy value can be obtained by combining Eqs. (20) and (21) as shown in Eq. (22):

$$\ln k_c = -\frac{\Delta H^0}{RT} + \frac{\Delta S^0}{R} \quad (22)$$

Where ΔG^0 is Gibbs free energy change (J/mol), ΔH^0 is the change in enthalpy (J/mol), ΔS^0 is the change in entropy (J/mol/K), R is a universal gas constant (8.314 J/mol K), T is the absolute temperature (K) and k_c is the equilibrium constant.^[40] The value of k_c can be calculated using Eq. (23):

$$k_c = \frac{q_e}{C_e} \quad (23)$$

The slope and intercept of the plot $\ln(k_c)$ versus $(1/T)$ give ΔH^0 and ΔS^0 , respectively. To determine the thermodynamics' parameters, batch adsorption studies were carried out at 10 mg/L MNZ concentration, at pH 7 and under three different temperatures (i.e., 293, 303 and 313 K).

2.8. Optimization of adsorption conditions by a central composite design

The effects of pH (x_1), temperature (x_2) and adsorbent dosage (x_3 ; either CG or PAC), i.e., effect of independent variables, on MNZ adsorption were evaluated by using a CCD. The ranges selected for the independent variables are as follows: $x_1 \sim 3\text{--}11$, $x_2 \sim 20\text{--}40^\circ\text{C}$ and $x_3 \sim 10\text{--}1,000$ mg/L. A three-factor full factorial CCD was constructed using Minitab 16 and the design is shown in Table 1. The effect of independent variables on MNZ adsorption was evaluated by calculating MNZ removal (Y_1 ; in %) and Gibbs free energy of adsorption Y_2 ; in J/mol). Using the experimental design, the experiments (Runs 1–20) were conducted in a batch mode with continuous shaking at an initial MNZ concentration of 10 mg/L for predetermined equilibrium time. At the end of the experiment, samples were collected and analyzed for MNZ concentration using HPLC. The center point was repeated six times to ensure the reproducibility of the experimental outcomes.

Table 1. The conditions of CCD experiments and the outcomes.

Run No.	pH	Temp ($^\circ\text{C}$)	Adsorbent dosage (mg/L)	MNZ removal (Y_1 , %)				ΔG° (Y_2 , J/mol)	
				PAC system		CG system		PAC system	CG system
				Exp	Pre	Exp	Pre		
1	7	30	505	93.00	92.75	22.33	23.86	-4,181.8	5,473.8
2	11	30	505	89.94	101.69	22.45	24.86	-3,184.5	5,455.4
3	3	30	505	98.65	105.50	23.38	25.68	-8,484.9	5,323.9
4	7	30	9	13.49	47.45	6.65	12.21	-3,130.3	-1,159.2
5	7	30	505	93.03	92.75	22.98	23.86	-4,194.3	5,380.7
6	7	30	1001	99.42	83.91	23.90	23.06	-8,901.8	6,975.2
7	7	30	505	93.07	92.75	23.27	23.86	-4,211.1	5,339.4
8	7	30	505	93.65	92.75	23.58	23.86	-4,444.7	5,295.1
9	9.4	36	210	96.51	79.51	21.88	19.94	-8,406.8	3,395.2
10	4.6	36	210	97.47	82.37	23.59	21.11	-9,251.8	3,145.4
11	7	20	505	91.21	102.72	21.89	24.69	-3,441.6	5,355.8
12	7	30	505	93.38	92.75	23.28	23.86	-4,332.7	5,337.2
13	4.6	24	210	97.62	80.82	22.52	19.58	-9,053.9	3,172.0
14	4.6	36	800	99.52	105.07	27.51	29.03	-10,127.2	6,050.9
15	9.4	36	800	99.20	102.54	25.27	28.20	-8,818.2	6,346.8
16	4.6	24	800	97.62	101.15	22.98	24.22	-5,751.3	6,409.8
17	7	30	505	94.06	92.75	23.01	23.86	-4,623.8	5,375.4
18	9.4	24	800	97.84	99.48	21.94	24.42	-5,991.8	6,557.5
19	9.4	24	210	97.84	78.83	21.65	19.43	-9,294.5	3,296.6
20	7	40	505	99.50	106.59	27.24	29.16	-11,341.2	4,967.3

Note: Exp—experimental values and Pre—predicted values based on the quadratic model obtained from CCD.

2.9. Desorption study

MNZ desorption from the adsorbents was evaluated using the adsorbents recovered (after carefully decanting the supernatant) at the end of the experiments from the equilibrium study. The flasks containing the adsorbents recovered from various systems (i.e., initial MNZ concentrations of 1, 5, 10, 50 and 100 mg/L) were added with 100-mL distilled water and kept in a temperature-controlled incubator shaker at 25°C for 24 h. The supernatant was withdrawn from flasks at the end of 24 h and analyzed for MNZ concentration. The difference in MNZ concentration, i.e., MNZ adsorbed in the adsorbents and in the supernatant after 24 h, was considered as an irreversible portion of MNZ from the adsorbent due to chemisorption.

3. Results and discussion

3.1. Effect of contact time and kinetics of MNZ adsorption

The effects of contact time on MNZ concentration and MNZ adsorption capacity in the presence of PAC and CG as adsorbents are shown in Figure 1a and b, respectively. It could be noticed in Figure 1 that MNZ adsorption on PAC was four times higher than CG at the end of 5 min of adsorption. In the PAC system, the calculated q_e was found to be 9.88 mg/g at the end of 5 min and no significant change was observed thereafter. The q_e profile in the CG system was similar to that of the PAC system; however, the value was nearly 45 times less compared to that of the PAC system. This could be due to the availability of large number of adsorption sites in PAC compared to CG.

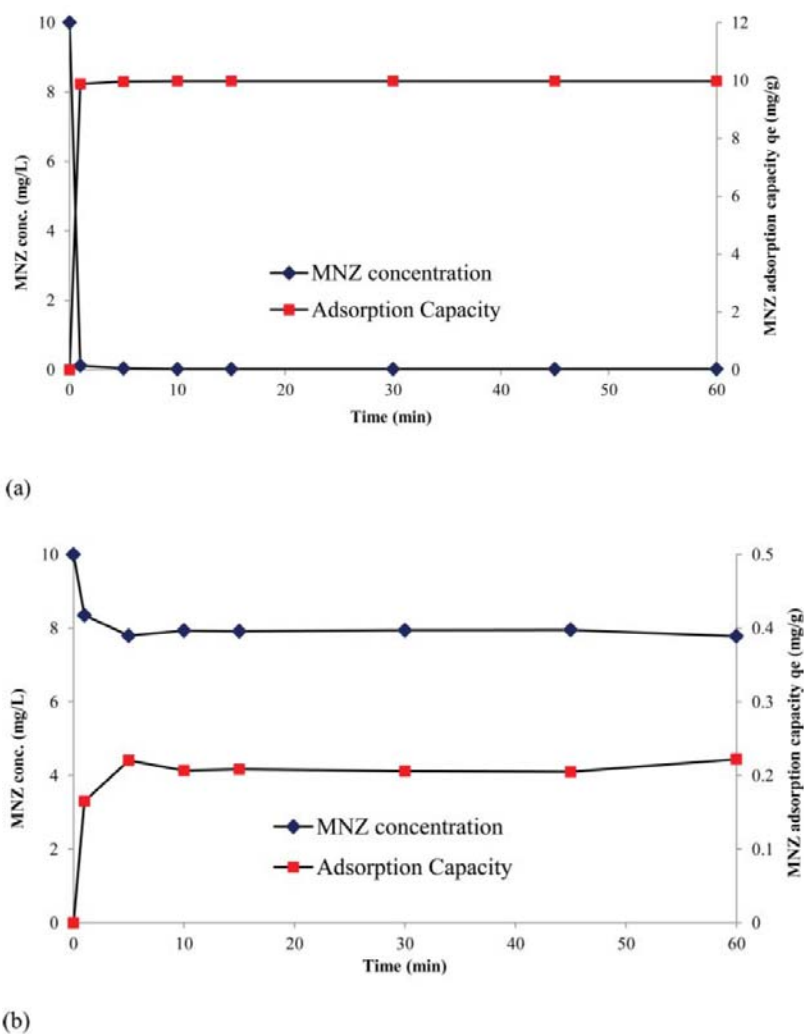


Figure 1. Effect of contact time on initial MNZ concentration on adsorption capacity (a) PAC (b) CG.

The order of reaction and reaction rate constant were found using Eqs. (3)–(6). The linearized plots of pseudo-first-order and pseudo-second-order models for both PAC and CG were prepared (Supporting information, Figures 2S and 3S); the rate constants were calculated and they are reported in Table 2. From the plots and Table 2, it was observed that the pseudo-second-order model was found to fit well the data of kinetic study. This shows that MNZ adsorption on both PAC and CG follows the second-order kinetics (R^2 of 1.00 and 0.997 for PAC and CG, respectively). On the other hand, the coefficient of determination for the pseudo-first-order model

was found to be very less for both PAC (0.368) and CG (0.264) adsorption systems. However, the values of the pseudo-second-order-kinetic constant (K_2) were found to be 16.73 and 7.98 g/mg/min for PAC and CG, respectively, which reveals that MNZ removal is rapid and spontaneous on PAC compared to CG. The calculated $q_e(q_{e-calc})$ values from the pseudo-second-order models (Supporting information; Table 1S) agreed well with the experimental $q_e(q_{e-exp})$ values of PAC and CG adsorption systems (Table 2). The goodness of fit of the pseudo-second-order model confirms that the kinetic sorption of MNZ on both PAC and CG is mainly due to chemisorption.

Table 2. Calculated values of kinetic and isotherm constants.

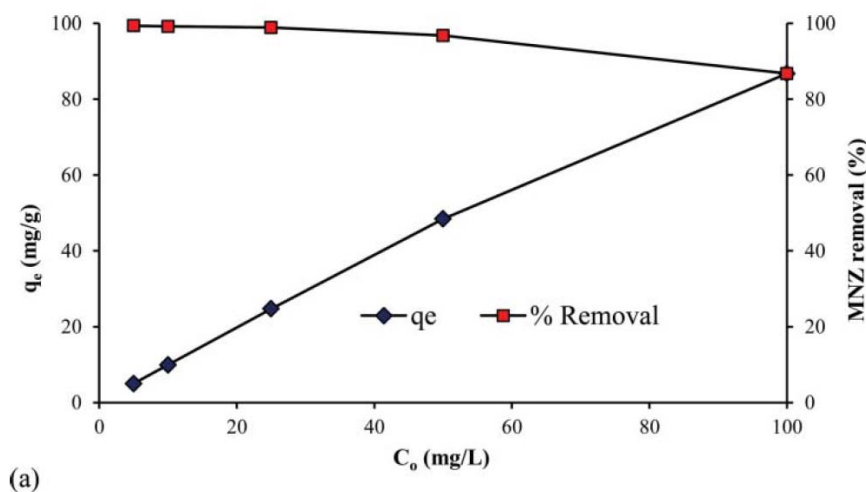
Model type	Model name	Parameters	PAC	R ²	CG	R ²
Kinetic model	Pseudo-first-order	q_{e-exp} (mg/g)	9.99	0.368	0.22	0.264
		q_{e-calc} (mg/g)	0.030		0.026	
		K_1 (min ⁻¹)	0.025		0.019	
	Pseudo-second-order	q_{e-exp} (mg/g)	9.99	1.00	0.22	0.997
		q_{e-calc} (mg/g)	9.98		0.21	
K_2 (g/mg/min)		16.73	7.98			
Isotherm model	Langmuir	q_m (mg/g)	54.35	0.991	0.076	0.659
		K_L (L/mg)	3.29		0.146	
	Freundlich	K_F	32.78	0.953	0.002	0.925
		$1/n$	0.4655		1.082	
	Temkin	A_T (L/mg)	30.60	0.977	0.1416	0.806
		B (J/mol)	13.646		3.123	
	Dubinin–Radushkevich	q_m (mg/g)	55.13	0.919	0.41	0.835
		K_{DR} (mol ² /kJ ²)	3.00E-8		2.00E-5	
	Elovich	E (kJ/mol)	4,082.48	0.994	223.60	0.396
		q_m (mg/g)	25.45		9.643	
K_E (L/mg)		9.137	1.740			

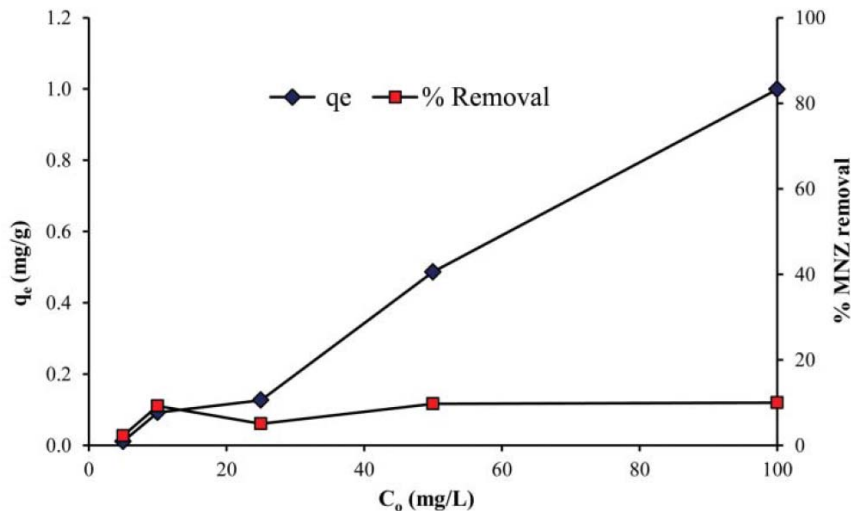
Note: q_{e-exp} is the experimental equilibrium adsorption capacity and q_{e-calc} is the calculated equilibrium adsorption capacity.

3.2. Equilibrium study

3.2.1 Effect of initial MNZ concentration

The effect of initial MNZ concentration on percentage removal and equilibrium adsorption capacity of PAC and CG in MNZ removal is shown in Figure 2a and b, respectively. It can be observed that the adsorption capacity of MNZ increased when the initial MNZ concentration also increased. This may be attributed to a higher probability of collision between the adsorbent and the adsorbate, which might have provided force to overcome the resistance of mass transfer of MNZ between aqueous and solid phases.^[41] The MNZ removal percentage in the PAC system decreased from 99% to 87% when the initial concentration increased from 5 mg/L to 100 mg/L. The decrease in MNZ removal could be attributed to the saturation of adsorption sites above a certain MNZ concentration.^[42]





(b)

Figure 2. Effect of initial MNZ concentration on adsorption capacity and % MNZ removal (a) PAC (b) CG.

3.2.2 Adsorption isotherm study

Using the experimental data of equilibrium study, the maximum MNZ adsorption capacities of PAC and CG were found using various isotherms listed in Table 2. The MNZ adsorption in PAC was fairly well fitted to all the isotherms ($R^2 > 0.9$), whereas the Freundlich isotherm was found to be more suitable to estimate the maximum MNZ adsorption capacity on CG (Supporting information, 4S–8S). It is worth noting in Table 2 that the R^2 value for the Langmuir isotherm was higher for PAC compared with other isotherms, indicating that MNZ removal occurred through monolayer adsorption. On the other hand, the value, i.e., R^2 , was higher for the Freundlich isotherm for CG systems. This indicates that the removal of CG was carried out by multilayer adsorption and the CG has a heterogeneous surface composed of different classes of adsorption sites. However, the $\frac{1}{n}$ value was found using the Freundlich isotherm for PAC (0.466) and CG (1.082), which specifies that adsorption of MNZ on PAC was more favorable compared with CG. A similar observation was found with other isotherm models as shown in Table 2. The plot of Temkin isotherm showed a better fit for the PAC system ($R^2 \sim 0.98$) than the CG system ($R^2 \sim 0.81$), indicating that it was due to the chemisorption process. The constant B obtained from the Temkin isotherm shows that heat of adsorption was higher for PAC (13.65) compared to CG (3.12). On the other hand, the Dubinin–Radushkevich isotherm constant q_m for PAC and CG was found to be 55.13 and 0.40 mg/g, respectively, indicating a better adsorption for PAC compared to CG for MNZ removal. Moreover, the Elovich isotherm represented the MNZ adsorption on PAC properly ($R^2 \sim 0.99$), whereas it was very poor in the case of CG ($R^2 \sim 0.40$). Therefore, the Elovich model cannot be used to properly interpret the MNZ adsorption on CG.

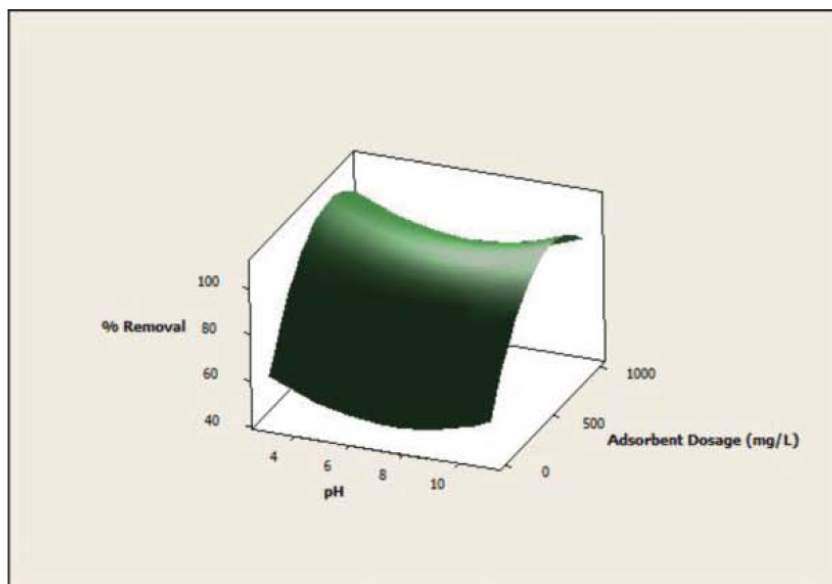
On the other hand, the favorability of the adsorption process was evaluated by calculating the dimensionless parameter (R_L) using Eq. (9). The R_L values were found to be in the range of 0.003–0.233 for PAC and 0.064–0.873 for CG when the initial MNZ concentration varied from 5 to 100 mg/L. The R_L values indicate that MNZ adsorption is favorable at different initial MNZ

concentrations. In addition, the mean free energy (E) for PAC and CG was calculated using Eq. (17) as 4,082.48 kJ/mol and 158.11 kJ/mol, respectively. The calculated values of E were much greater than 16 kJ/mol, indicating that the adsorption mainly occurred by chemisorption.^[38] The aforementioned observations, i.e., values of $\frac{1}{n}$, R_L and E, indicate that chemisorption was responsible for MNZ adsorption on both PAC and CG. Therefore, the maximum MNZ adsorption capacity of PAC was speculated to be between 25.45 and 32.78 mg/g as three isotherms predicted (based on a chemisorption approach) a similar adsorption capacity range in the PAC systems. On the other hand, the adsorption capacity of CG was found to be in the range of 0.41–0.002 mg/g (Table 2).

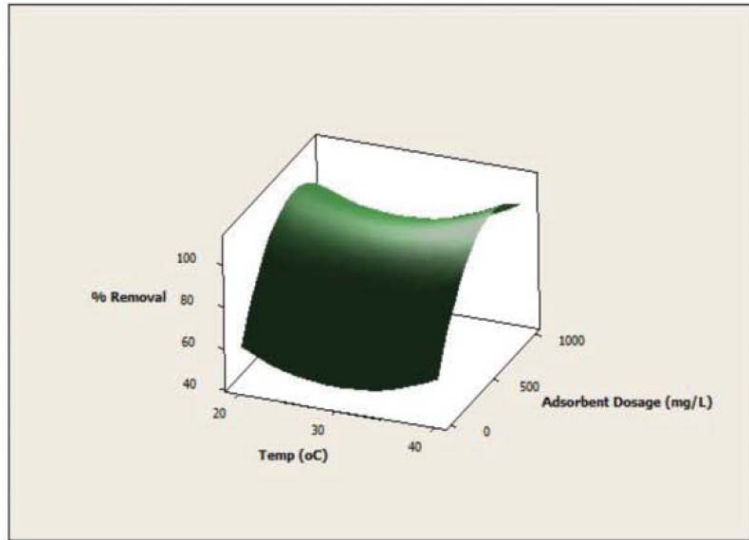
3.3. Outcomes of CCD experiments

3.3.1 Effect of pH, temperature and adsorbent dosage on MNZ removal

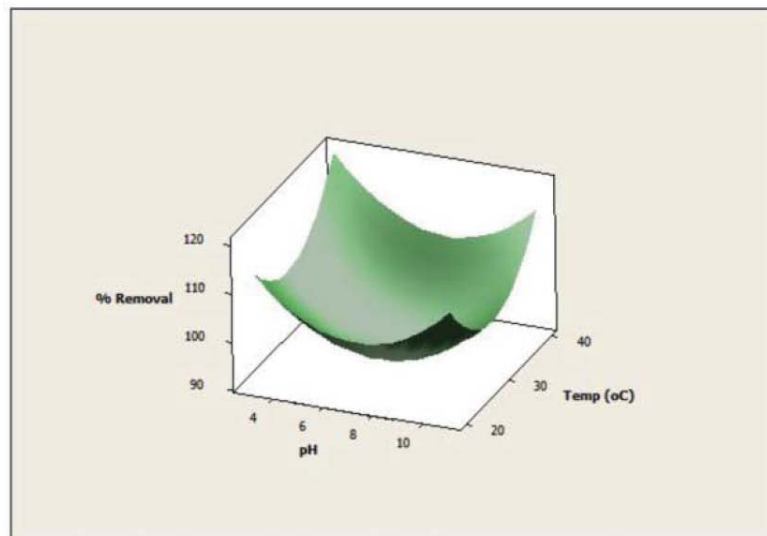
The outcomes of CCD experiments are shown in Table 1. The response surfaces showing the effect of (i) adsorbent dosage and pH, (ii) adsorbent dosage and temperature and (iii) pH and temperature on MNZ removal in the PAC system are presented in Figures 3a–c and 4a–c, respectively. It can be observed that the increase in adsorbent dosage at any pH range shows an increase in MNZ removal (Figs. 3a and 4a). This can be attributed to the fact that increasing adsorbent dosage increases the surface area and number of active sites of the adsorbent.^[41] The pH of the solution has not shown any major effect on changing the adsorbent dosage required for MNZ removal. Rivera et al.^[43] reported a similar conclusion based on the removal of nitroimidazole by adsorption on activated carbon.



(a)



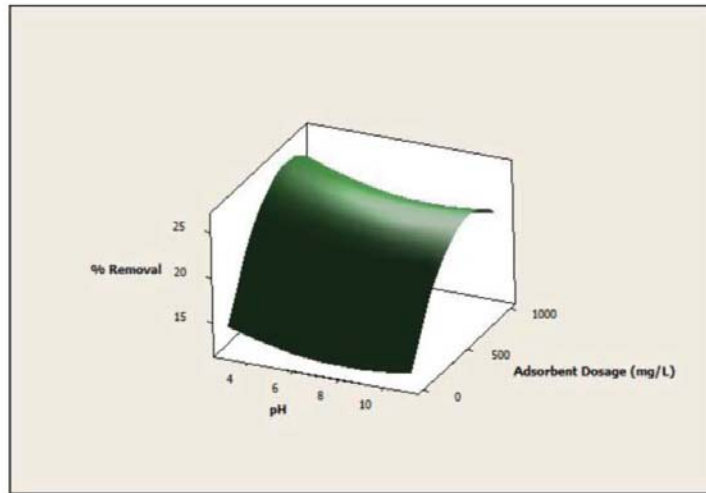
(b)



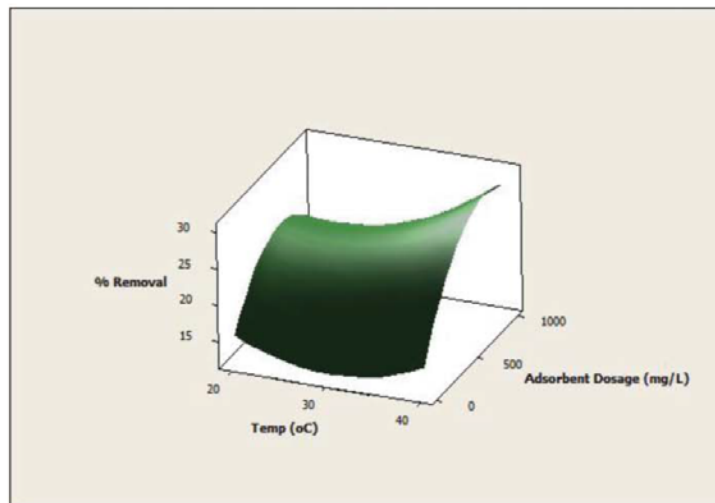
(c)

Figure 3. Effect of (a) adsorbent dosage and pH, (b) adsorbent dosage and temperature and (c) pH and temperature on MNZ removal by adsorption in the PAC system.

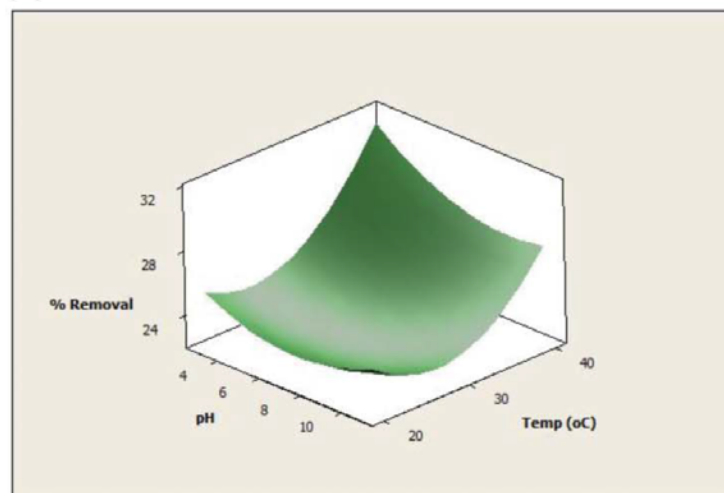
Figures 3b and 4b show the response surface plots of adsorbent dosage and temperature on MNZ removal in PAC and CG systems, respectively. The maximum removal was found to be at higher temperature and at higher adsorbent dosage in both PAC and CG. The increase in MNZ removal with the increase in temperature may be due to the enlargement of pore size of adsorbent, surface activation, increase in mobility of adsorbate ions and reduced swelling effect of adsorbent.^[37] On the other hand, MNZ removal was found to be very less at neutral pH at 30°C compared with highly acidic and highly alkaline pH conditions (Fig. 3c). A similar trend was observed in the CG system, i.e., the percentage MNZ removed was found to be higher in acidic pH at a higher temperature (Fig. 4c).



(a)



(b)



(c)

Figure 4. Effect of (a) adsorbent dosage and pH, (b) adsorbent dosage and temperature and (c) pH and temperature on MNZ removal by adsorption in the CG system.

The empirical relationship between the three independent variables and response can be represented by a generic equation as given in Eq. (24), where Y is a response and x_{ij} represents independent variables. A second-order quadratic model was obtained using the CCD data as shown in Eqs. (24) and (25), which gives the empirical relationship between the independent variables (x_1 , x_2 and x_3) and the MNZ removal (dependent variable, i.e., Y) for PAC and CG, respectively. These equations can be used to calculate a set of combinations of x_1 , x_2 and x_3 for a predetermined Y value, which will be useful in real-time operations.

$$Y = b_0 + \sum b_i x_i + \sum b_{ii} x_i^2 + \sum b_{ij} x_i x_j \quad (24)$$

$$\begin{aligned} Y_{PAC} = & 183.8300 - 9.3976x_1 - 6.8853x_2 + 0.1369x_3 \\ & + 0.6654x_1^2 + 0.1169x_2^2 - 0.0001x_3^2 - 0.0149x_1x_2 \\ & + 0.0001x_1x_3 + 0.0003x_2x_3 \end{aligned} \quad (25)$$

$$\begin{aligned} Y_{CG} = & 40.9737 - 0.8443x_1 - 1.6914x_2 + 0.0217x_3 \\ & + 0.0865x_1^2 + 0.0300x_2^2 - 0.00003x_3^2 \\ & - 0.0177x_1x_2 + 0.0001x_1x_3 + 0.0005x_2x_3 \end{aligned} \quad (26)$$

where b_0 , b_i , b_{ii} and b_{ij} are the constants obtained from the model, Y_{PAC} and Y_{CG} represent the MNZ removal by PAC and CG, respectively.

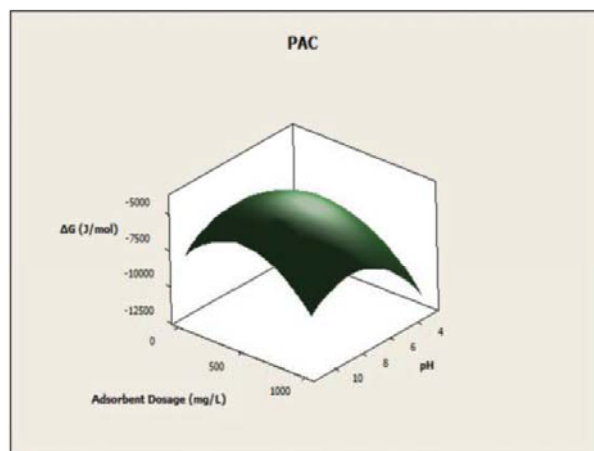
3.3.2 Variation of Gibbs free energy with adsorbent dosage, temperature and pH

Figure 5a–f shows the surface plots of ΔG^0 with respect to interaction between adsorbent dosage, pH and temperature for PAC and CG, respectively. In Figure 5a, ΔG^0 was the lowest (more negative) at pH 4 and at an adsorbent dosage of 1,000 mg/L, which indicate that the MNZ adsorption is highly spontaneous in the PAC system. On the other hand, ΔG^0 decreased as adsorbent dosage decreased and pH showed no significant effect on ΔG^0 in the CG system (Fig. 5b). In Figure 5c, ΔG^0 was more negative at 40°C and adsorbent dosage of 1,000 mg/L in the PAC system, whereas ΔG^0 decreased as adsorbent dosage decreased and temperature showed much less significant effect on ΔG^0 value in the CG system (Fig. 5d). For PAC, ΔG^0 was more negative at pH 4 and at 40°C (Fig. 5e). On the other hand, the lower value of ΔG^0 can be noticed at pH 4 and at 40°C for CG (Fig. 5f). Overall, higher adsorbent dosage at acidic pH and at higher temperature makes the adsorption process more feasible and spontaneous for PAC.

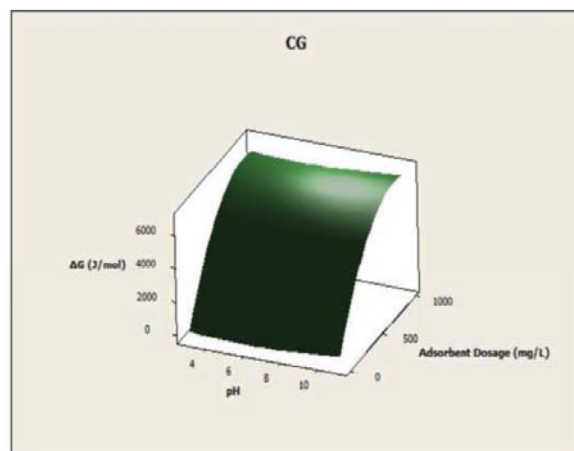
3.3.3 Optimization of operating conditions

The suitable operational conditions/combinations, i.e., adsorbent dosage, temperature and pH, for almost complete MNZ removal by PAC were analyzed using the response optimizer function in Minitab. The different operationally suitable combinations of adsorbent dosage, temperature and pH for complete MNZ removal using PAC as adsorbent are shown in Table 3. On the other hand, only 86.7% of MNZ removal was observed in the kinetic study when the experiment was conducted at 10 mg/L MNZ, pH 7 and at 25°C with 1,000 mg/L PAC dosage. The increase in system's temperature from 25°C to 36°C and 40°C could completely remove MNZ at much lower dosages.

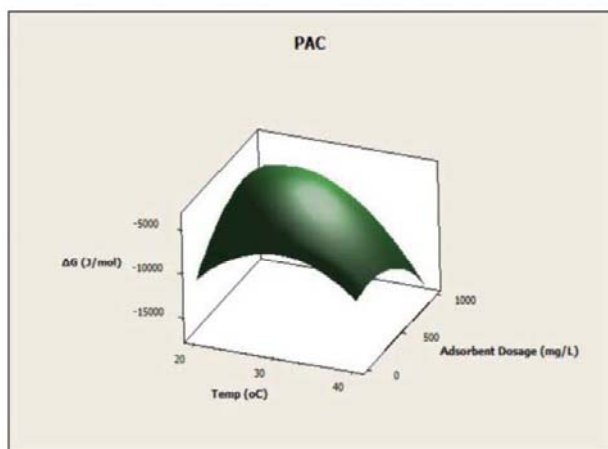
Nearly 62% less adsorbent dosage is required and moreover complete MNZ removal could be achieved at the elevated temperature.



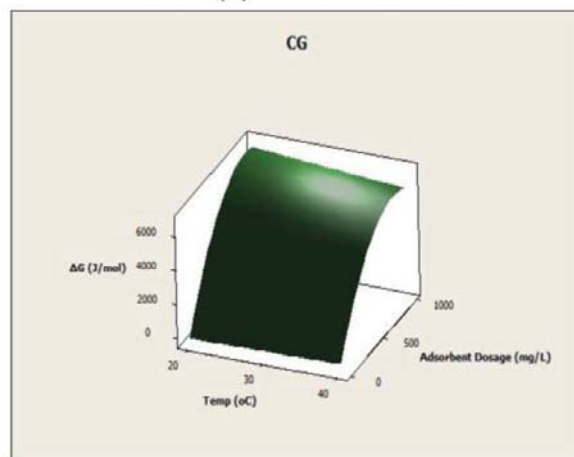
(a)



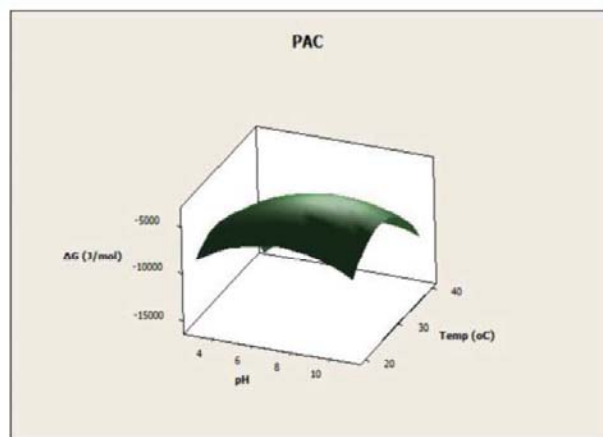
(b)



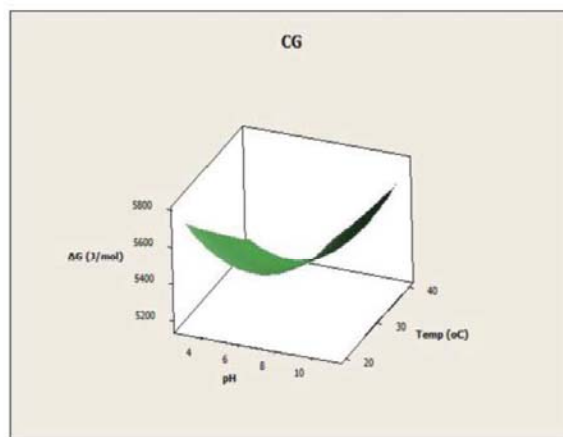
(c)



(d)



(e)



(f)

Figure 5. (a–f) Three-dimensional surface plot of variation of ΔG^0 with respect to interaction between adsorbent dosage pH and temperature for PAC and CG.

Table 3. Operating conditions for complete MNZ removal in the PAC adsorption system.

MNZ concentration (mg/L)	pH	Temperature (°C)	Adsorbent dosage (mg/L)	Removal (%)
10	7	36	800	100
		39.5	400	
		40	384	
		25	1,000	
				86.7

3.4. Correlation of MNZ adsorption and thermodynamic parameters

The correlation between temperature and MNZ removal was analyzed by estimating the thermodynamic parameters using Eqs. (20)–(23). The calculation of thermodynamic parameters is possible based on the constants from Langmuir, Frumkin, Flory–Huggins, Liu isotherms and also from thermodynamic equilibrium constant as shown in Eq. (23). However, k_c was calculated based on Eq. (23) and the observations of thermodynamic parameters with respect to change in temperature were in good agreement with the earlier observations.^[44] However, the thermodynamic parameters can also be calculated based on the Langmuir constant for organic compounds with weak charges like MNZ as suggested by Liu.^[45]

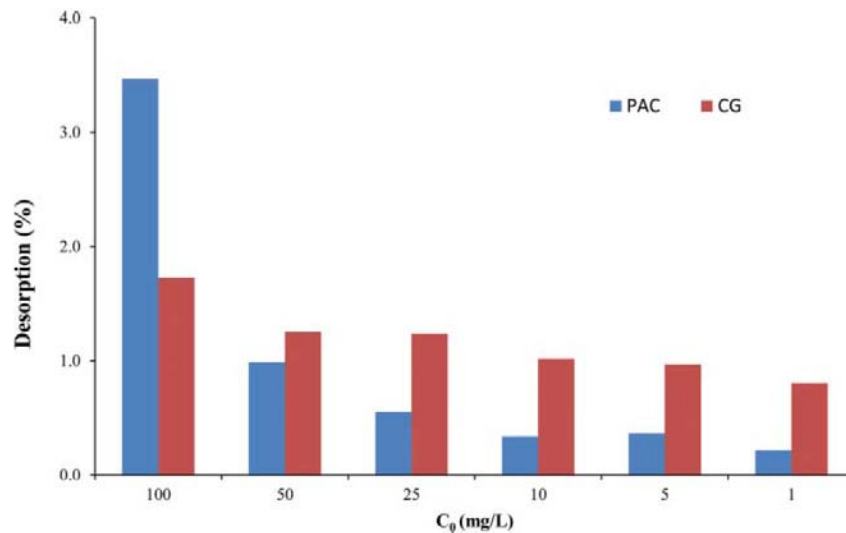
The calculated values of k_c , ΔG^0 , ΔH^0 and ΔS^0 based on thermodynamic equilibrium constants considering weak charges of MNZ are shown in Table 4. The values of ΔH^0 and ΔS^0 were found to be positive for both PAC and CG, whereas the ΔG^0 value was negative for PAC and positive for CG. The negative ΔG^0 value for PAC indicates that the adsorption process is thermodynamically feasible and spontaneous in nature, whereas the positive ΔG^0 value for CG indicates the non-spontaneous nature of MNZ adsorption. For PAC and CG, the value of ΔG^0 decreases as temperature increases, suggesting that higher temperature favors the adsorption process. However, the positive ΔH^0 value for both PAC and CG indicates that the adsorption process is endothermic in nature. The adsorption process in the solid–liquid system is a combination of two processes, i.e., desorption of previously adsorbed water molecules from adsorbent surface and adsorption of adsorbate species. For MNZ adsorption on the adsorbent surface, MNZ ions have to replace more than one water molecule, which would have resulted in the adsorption process being endothermic.^[46] An endothermic process obtains its energy in the form of heat from surrounding molecules/environment, which could be unequivocally attributed to the chemisorption process.^[47] At the same time, the positive ΔS^0 value for PAC and CG indicates increased randomness at the solid–solution interface during the fixation of MNZ ions on active sites of adsorbents.^[48] Thus, an increase in MNZ adsorption was observed at higher temperatures. The whole outcome of adsorption experiments reveals that MNZ adsorption by CG (with a graphene content of 2% w/w) is insignificant compared to the removal by PAC. However, MNZ removal in the CG system could be improved by increasing the graphene content of concrete. However, the cost required and uniformity in adsorbent preparation would be the likely challenges, which needs a detailed investigation.

Table 4. Thermodynamic constants of PAC and CG for MNZ removal.

Adsorbent	Temperature (K)	k_c	ΔG° (J/mol)	ΔH° (J/mol)	ΔS° (J/mol/K)	R^2
PAC	293	4.11	-3,441.6	111548	389.5	0.843
	303	6.27	-6,465.3			
	313	78.11	-11,341.2			
CG	293	0.11	5,376.92	11014	19.17	0.962
	303	0.12	5,341.2			
	313	0.15	4,936.8			

3.5. Desorption study

The desorption study helps to explain the mechanism of adsorption process.^[48-50] An adsorbate's weak association with the adsorbent could be removed by water (i.e., universal solvent), which is an indication of weak bonds during the adsorption process. On the other hand, the removal that could be possible by strong base/strong acid or by organic acids is an indication of adsorption by the exchange of ions or chemisorption process, respectively. Figure 6 shows the percentage of MNZ desorbed from the surface of PAC and CG after 24 h. A maximum of 3.5% and 1.7% MNZ desorption was observed in the PAC and CG systems, respectively. The very low MNZ desorption by distilled water from PAC and CG systems indicates that some complexes may have formed between active sites of adsorbents and MNZ species. However, strong acidic solvents (HCl, H₂SO₄ and HNO₃), strong basic solvents (NaOH) and organic acids (CH₃COOH) may promote the MNZ recovery and the regeneration of adsorbents.

**Figure 6.** MNZ desorption from PAC and CG adsorption systems.

4. Conclusions

Batch-mode MNZ adsorption experiments were carried out using PAC and CG. The MNZ adsorption capacity of PAC was 45 times higher compared to CG. Adsorption of MNZ on both PAC and CG followed the pseudo-second-order kinetic model. The increase in the system's temperature (20–40°C) ensured complete removal of MNZ at a much lower dosage of PAC. Thermodynamic parameters indicated that MNZ adsorption on PAC was spontaneous and endothermic. On the other hand, the MNZ removal was non-spontaneous and endothermic on CG. The outcome of adsorption experiments pointed out that MNZ removal by CG was insignificant compared to PAC. The quantity of MNZ desorbed from PAC and CG was very low with distilled water, which indicated the formation of complexes during chemisorption. The application of solvents and/or other acidic reagents could be useful for MNZ recovery. As a whole, PAC and CG with more graphene content could be useful in treating water and wastewater containing MNZ and other similar compounds.

Acknowledgements

The authors are grateful to the research collaboration between IIT Madras and University of Technology Sydney.

Funding

The authors acknowledge the financial support provided by the Centre for Industrial Consultancy and Sponsored Research (ICSR), IIT Madras, which made this research study (Grant No: CIE/14–15/832/NFIG/SMAT and CIE/14–15/650/NFSC/SMAT) possible.

Supplementary Materials

Supplementary data related to this article can be found at <http://orcid.org/0000-0002-4124-4605>.

References

- [1] Liu, J.L.; Wong, M.-H. Pharmaceuticals and personal care products (PPCPs): A review on environmental contamination in China. *Environ. Int.* 2013, 59, 208–224.
- [2] Lanzky, P.F.; Haning-Sorensen, B. The toxic effect of the antibiotic metronidazole on aquatic organisms. *Chemosphere* 1997, 35, 2553–2561.
- [3] Manamsa, K.; Crane, E.; Stuart, M.; Talbot, J.; Lapworth, D.; Hart, A. A national-scale assessment of micro-organic contaminants in groundwater of England and Wales. *Sci. Total Environ.* 2016, 568, 712–726.
- [4] Phillips, P.J.; Schubert, C.; Argue, D.; Fisher, I.; Furlong, E.T.; Foreman, W.; Gray, J.; Chalmers, A. Concentrations of hormones, pharmaceuticals and other micropollutants in groundwater affected by septic systems in New England and New York. *Sci. Total Environ.* 2015, 512–513, 43–54.
- [5] Vulliet, E.; Cren-Oliv_e, C. Screening of pharmaceuticals and hormones at the regional scale, in surface and groundwaters intended to human consumption. *Environ. Pollut.* 2011, 159, 2929–2934.
- [6] Cabeza, Y.; Candela, L.; Ronen, D.; Teijon, G. Monitoring the occurrence of emerging contaminants in treated wastewater and groundwater between 2008 and 2010. The Baix Llobregat (Barcelona, Spain). *J. Hazard. Mater.* 2012, 239–240, 32–39.

- [7] K'oreje, K.O.; Vergeynst, L.; Ombaka, D.; De Wispelaere, P.; Okoth, M.; Van Langenhove, H.; Demeestere, K. Occurrence patterns of pharmaceutical residues in wastewater, surface water and groundwater of Nairobi and Kisumu city, Kenya. *Chemosphere* 2016, 149, 238–244.
- [8] Ammar, H.B.; Brahim, M.B.; Abdelhédi, R.; Samet, Y. Green electrochemical process for metronidazole degradation at BDD anode in aqueous solutions via direct and indirect oxidation. *Sep. Purif. Technol.* 2016, 157, 9–16.
- [9] Fang, Z.; Chen, J.; Qiu, X.; Qiu, X.; Cheng, W.; Zhu, L. Effective removal of antibiotic metronidazole from water by nanoscale zerovalent iron particles. *Desalination*. 2011, 268, 60–67.
- [10] Rosal, R.; Rodríguez, A.; Perdígón-Melón, J.A.; Petre, A.; García-Calvo, E.; Gómez, M.J.; Aguera, A.; Fernandez-Alba, A.R. Occurrence of emerging pollutants in urban wastewater and their removal through biological treatment followed by ozonation. *Water Res.* 2010, 44, 578–588.
- [11] Kümmerer, K.; Al-Ahmad, A.; Mersch-Sundermann, V. Biodegradability of some antibiotics, elimination of the genotoxicity and affection of wastewater bacteria in a simple test. *Chemosphere* 2000, 40, 701–710.
- [12] Chianeh, F.N.; Parsa, J.B. Electrochemical degradation of metronidazole from aqueous solutions using stainless steel anode coated with SnO₂ nanoparticles: Experimental design. *Rev. Mex. Urol.* 2016, 76, 424–432.
- [13] Dong, S.; Sun, J.; Li, Y.; Yu, C.; Li, Y.; Sun, J. ZnSnO₃ hollow nanospheres/reduced graphene oxide nanocomposites as high-performance photocatalysts for degradation of metronidazole. *Appl. Catal. B Environ.* 2014, 144, 386–393.
- [14] Saidi, I.; Soutrel, I.; Fourcade, F.; Amrane, A.; Bellakhal, N.; Geneste, F. Electrocatalytic reduction of metronidazole using titanocene/Nafion®-modified graphite felt electrode. *Electrochim. Acta.* 2016, 191, 821–831.
- [15] Yang, J.; Zhu, M.; Wang, X.; Alvarez, P.J.J.; Liu, K. Poly(vinylidene fluoride) membrane supported nano zero-valent iron for metronidazole removal: Influences of calcium and bicarbonate ions. *J. Taiwan Inst. Chem. Eng.* 2015, 49, 113–118.
- [16] Ammar, H.B.; Brahim, M.B.; Abdelhédi, R.; Samet, Y. Enhanced degradation of metronidazole by sunlight via photo-Fenton process under gradual addition of hydrogen peroxide. *J. Mol. Catal. A Chem.* 2016, 420, 222–227.
- [17] Saidi, I.; Soutrel, I.; Floner, D.; Fourcade, F.; Bellakhal, N.; Amrane, A.; Geneste, F. Indirect electroreduction as pretreatment to enhance biodegradability of metronidazole. *J. Hazard. Mater.* 2014, 278, 172–179.
- [18] Foo, K.Y.; Hameed, B.H. Insights into the modeling of adsorption isotherm systems. *Chem. Eng. J.* 2010, 156, 2–10.
- [19] Rangabhashiyam, S.; Nandagopal, M.S.G.; Nakkeeran, E.; Selvaraju, N. Adsorption of hexavalent chromium from synthetic and electroplating effluent on chemically modified Swietenia mahagoni shell in a packed bed column, *Environ. Monit. Assess.* 2016, 188, 1–13.
- [20] Nitivattananon, V.; Borongan, G. Construction and demolition waste management: Current practices in Asia. *Proceedings of the International Conference on Sustainable Solid Waste Management*, 5–7 Sept, Chennai, India, 2007, 97–104.
- [21] Wang, X.; Chen, J.; Kong, Y.; Shi, X. Sequestration of phosphorus from wastewater by cement-based or alternative cementitious materials. *Water Res.* 2014, 62, 86–96.

- [22] Jo, M.; Soto, L.; Arocho, M.; St John, J.; Hwang, S. Optimum mix design of fly ash geopolymer paste and its use in pervious concrete for removal of fecal coliforms and phosphorus in water. *Constr. Build. Mater.* 2015, 93, 1097–1104.
- [23] Wang, Z.; Chen, Z.; Chang, J.; Shen, J.; Kang, J.; Chen, Q. Fabrication of a low-cost cementitious catalytic membrane for p-chloronitrobenzene degradation using a hybrid ozonation-membrane filtration system. *Chem. Eng. J.* 2015, 262, 904–912.
- [24] De-Andrade, F.V.; De-Lima, G.M.; Augusti, R.; Da-Silva, J.C.C.; Coelho, M.G.; Paniago, R.; Machado, I.R. A novel TiO₂/autoclaved cellular concrete composite: From a precast building material to a new floating photocatalyst for degradation of organic water contaminants. *J. Water. Process. Eng.* 2015, 7, 27–35.
- [25] Ok, Y.S.; Yang, J.E.; Zhang, Y.S.; Kim, S.J.; Chung, D.Y. Heavy metal adsorption by a formulated zeolite-portland cement mixture. *J. Hazard. Mater.* 2007, 147, 91–96.
- [26] Karkar, S.; Debnath, S.; De, P.; Parashar, K.; Pillay, K.; Sashikumar, P.; Ghosh, U.C. Preparation, characterization and evaluation of fluoride adsorption efficiency from water of ironaluminium oxide-graphene oxide composite material. *Chem. Eng. J.* 2016, 306, 269–279.
- [27] Nam, S.W.; Jung, C.; Li, H.; Yu, M.; Flora, J.R.V.; Boateng, L.K.; Her, N.; Zoh, K.D.; Yoon, Y. Adsorption characteristics of diclofenac and sulfamethoxazole to graphene oxide in aqueous solution. *Chemosphere* 2015, 136, 20–26.
- [28] Qi, Y.; Yang, M.; Xu, W.; He, S.; Men, Y. Natural polysaccharides-modified graphene oxide for adsorption of organic dyes from aqueous solutions. *J. Colloid. Interface Sci.* 2017, 486, 84–96.
- [29] Tan, P.; Hu, Y.; Bi, Q. Competitive adsorption of Cu²⁺, Cd²⁺ and Ni²⁺ from an aqueous solution on graphene oxide membranes. *Colloids Surf A Physicochem. Eng. Asp.* 2016, 509, 56–64.
- [30] Rodrigues, A.E.; Silva, C.M. What's wrong with Lagergren pseudo first order model for adsorption kinetics? *Chem. Eng. J.* 2016, 306, 1138–1142.
- [31] Ho, Y.S.; McKay, G. The kinetics of sorption of divalent metal ions onto Sphagnum moss peat. *Water Res.* 2000, 34, 735–742.
- [32] Ho, Y.S.; McKay, G. Pseudo second order model for sorption processes. *Process Biochem.* 1999, 34, 451–465.
- [33] Rangabhashiyam, S.; Anu, N.; Giri-Nandagopal, M.S.; Selvaraju, N. Relevance of isotherm models in biosorption of pollutants by agricultural byproducts. *J. Environ. Chem. Eng.* 2014, 2, 398–414.
- [34] Langmuir, I. The Constitution and fundamental properties of solids and liquids. Part I. Solids. *J. Am. Chem. Soc.* 1916, 38, 2221–2295.
- [35] Freundlich, H.; Heller, W. The Adsorption of cis- and trans-Azobenzene. *J. Am. Chem. Soc.* 1939, 61, 2228–2230.
- [36] Temkin, M.J.; Phyzev, V. Recent modifications to Langmuir isotherms. *Acta Physico-Chimica USSR.* 1940, 12, 217–222.
- [37] Rangabhashiyam, S.; Selvaraju, N. Evaluation of the biosorption potential of a novel *Caryota urens* inflorescence waste biomass for the removal of hexavalent chromium from aqueous solutions. *J. Taiwan Inst. Chem. Eng.* 2015, 47, 59–70.
- [38] Ghasemi, M.; Naushad, M.; Ghasemi, N.; Khosravi-fard, Y. Adsorption of Pb(II) from aqueous solution using new adsorbents prepared from agricultural waste: adsorption isotherm and kinetic studies. *J. Ind. Eng. Chem.* 2014, 20, 2193–2199.

- [39] Hamdaoui, O.; Naffrechoux, E. Modeling of adsorption isotherms of phenol and chlorophenols onto granular activated carbon. Part I. Two-parameter models and equations allowing determination of thermodynamic parameters. *J. Hazard. Mater.* 2007, 147, 381–394.
- [40] Rangabhashiyam, S.; Nakkeeran, E., Anu, N., Selvaraju, N. Biosorption potential of a novel powder, prepared from *Ficus auriculata* leaves, for sequestration of hexavalent chromium from aqueous solutions. *Res. Chem. Intermed.* 2015, 41, 8405–8424.
- [41] Srivastava, V.C.; Swamy, M.M.; Mall, I.D.; Prasad, B.; Mishra, I.M. Adsorptive removal of phenol by bagasse fly ash and activated carbon: equilibrium, kinetics and thermodynamics. *Colloids Surf. A Physicochem. Eng. Asp.* 2006, 272, 89–104.
- [42] Singh, R.K.; Kumar, S.; Kumar, S.; Kumar, A. Development of parthenium based activated carbon and its utilization for adsorptive removal of p-cresol from aqueous solution. *J. Hazard. Mater.* 2008, 155, 523–535.
- [43] Rivera-Utrilla, J.; Prados-Joya, G.; Sánchez-Polo, M.; Ferro-García, M.A.; Bautista-Toledo, I. Removal of nitroimidazole antibiotics from aqueous solution by adsorption/bioadsorption on activated carbon. *J. Hazard. Mater.* 2009, 170, 298–305.
- [44] Liu, Y.; Xu, H. Equilibrium, thermodynamics and mechanisms of Ni^{2+} biosorption by aerobic granules. *Biochem. Eng. J.* 2007, 35, 174–182.
- [45] Liu, Y. Is the free energy change of adsorption correctly calculated? *J. Chem. Eng. Data* 2009, 54, 1981–1985.
- [46] Rawat, V.; Rai, P.; Gautam, R.K.; Chattopadhyaya, M.C. Kinetic and equilibrium isotherm studies for the adsorptive removal of brilliant green dye from aqueous solution by *Oplismenus frumentaceus* husk. *J. Indian Chem. Soc.* 2013, 90, 577–583.
- [47] Tran, H.N.; You, S.J.; Chao, H.P. Thermodynamic parameters of cadmium adsorption onto orange peel calculated from various methods: A comparison study. *J. Environ. Chem. Eng.* 2016, 4, 2671–2682.
- [48] Lataye, D.H.; Mishra, I.M.; Mall, I.D. Removal of 4-Picoline from aqueous solution by adsorption onto bagasse fly ash and rice husk ash: Equilibrium, thermodynamic, and desorption study. *J. Environ. Eng.* 2011, 137, 1048–1057.
- [49] Kumar, M.; Philip, L. Adsorption and desorption characteristics of hydrophobic pesticide endosulfan in four Indian soils. *Chemosphere* 2006, 62, 1064–1077.
- [50] Rangabhashiyam, S.; Selvaraju, N. Efficacy of unmodified and chemically modified *Swietenia mahagoni* shells for the removal of hexavalent chromium from simulated wastewater. *J. Mol. Liq.* 2015, 209, 487–497.
- [51] Mall, I.D.; Srivastava, V.C.; Kumar, G.V.A.; Mishra, I.M. Characterization and utilization of mesoporous fertilizer plant waste carbon for adsorptive removal of dyes from aqueous solution. *Colloids Surf. A Physicochem. Eng. Asp.* 2006, 278, 175–187.